Sustainable Energy & Fuels

Phenylene-bridged perylenediimide-porphyrin acceptors for non-fullerene organic solar cells

Journal:	*Sustainable Energy & Fuels*
Manuscript ID	SE-ART-08-2018-000427.R1
Article Type:	Paper
Date Submitted by the Author:	05-Sep-2018

Complete List of Authors:	Zhang, Quanquan; China University of Geosciences, Faculty of Materials Science and Chemistry Xu, Xiaopeng; Sichuan University, Department of Chemistry Chen, Song; Hong Kong Baptist University, Department of Chemistry Bodedla, Govardhana Babu; Hong Kong Baptist University, Chemistry Sun, Mingzi; The Hong Kong Polytechnic University, Department of Applied Biology and Chemical Technology Hu, Qin; Materials Sciences Division, Lawrence Berkeley National Lab, Berkeley Peng, Qiang; Sichuan University, Department of Chemistry Huang , Bolong; Hong Kong Polytechnic University Faculty of Applied Sciences and Textiles, Applied Biology and Chemical Technology Ke, Hanzhong; China University of Geosciences, Faculty of Materials Science and Chemistry Liu, Feng; Shanghai Jiao Tong University Russell, Thomas; University of Massachusetts Zhu, Xunjin; Hong Kong Baptist University, Chemistry

Phenylene-bridged perylenediimide-porphyrin acceptors for non-fullerene organic solar cells

Quanquan Zhang,[a, b]‡ Xiaopeng Xu,[c]‡ Song Chen,[b]‡ Govardhana Babu Bodedla,[b] Mingzi Sun,[d] Qin Hu,[f] Qiang Peng,[c] Bolong Huang,[d] Hanzhong Ke,*[a] Feng Liu,*[e] Thomas P. Russell,[f] Xunjin Zhu*[b]*

[a] *Faculty of Material Science and Chemistry, China University of Geosciences, Wuhan, Hubei 430074, P. R. China. E-mail: kehanz@aliyun.com*

[b] *Department of Chemistry and Institute of Molecular Functional Materials, Hong Kong Baptist University, Waterloo Road, Kowloon Tong, Hong Kong, P. R. China. E-mail: xjzhu@hkbu.edu.hk*

[c] *Department of Chemistry, Sichuan University, Chengdu, Sichuan 610000, P. R. China. Email: qiangpeng@scu.edu.cn*

[d] *Department of Applied Biology & Chemical Technology, The Hong Kong Polytechnic University, Hung Hom, Hong Kong, P. R. China*

[e] *Department of Physics and Astronomy, and Collaborative Innovation Center of IFSA, Shanghai Jiao Tong University, Shanghai, 200240, P. R. China. E-mail: fengliu82@sjtu.edu.cn*

[f] *Department of Polymer Science and Engineering, University of Massachusetts, Amherst, MA, 01003, U.S.A.*

ABSTRACT: New perylenediimide-porphyrin acceptors, 4PDI-ZnP and 2PDI-ZnP have been facilely synthesized by the acid-catalyzed condensation of perylenediimide-substituted benzaldehyde with respective dipyrromethance and pyrrole, and subsequent Zn(II)-complexation. The 4PDI-ZnP with four perylenediimide (PDI) moieties appended onto the zinc(II)-porphyrin core shows higher electon mobility than 2PDI-ZnP with only two PDI units. And the π-conjugation between the PDI and porphyrin is significantly weakened by the phenylene linkage twisted to them due to the steric hindrance, which renders them an undisturbed absorption features from porphyrin and PDI in a range of 385–600 nm. For their spectral absorption properties perfect complementary to the common polymer donor, PTB7-Th, the two acceptors have been evaluated together with PTB7-Th for non-fullerene bulk heterojunction organic solar cells (BHJ OSCs). High power conversion efficiency of 9.64% has been achieved using the blend of 4PDI-ZnP:PTB7-Th for its optimal visible sunlight harvesting, favorable morphological properties and efficient charge dissociation upon photon absorption. This represents hitherto benchmark photovoltaic peformance for PDI acceptors and PTB7-Th donor systems. It should be noted that the porphyrin core not only act as scaffold for PDI moieties, but also contribute the light-harvesting in near-ultraviolet and violet regions, which is unambiguously demonstrated in single-component BHJ OSCs based on the two acceptors.

KEYWORDS: Porphyrin, perylenediimide, phenylene-bridged, non-fullerene acceptor, heterojunction organic solar cells

INTRODUCTION

Bulk heterojunction organic solar cells (BHJ OSCs) with active layers comprising an electron donor and an electron acceptor have been extensively studied owing to their solution

processability, materials tunability, and appealing lightweight and flexible device characteristics. Solution processability enables high-throughput roll-to-roll fabrication leading to potentially low-cost manufacturing, while materials tunability permits modulation of molecular energetics and spectral properties for optimal donor-acceptor energetic matching and efficient solar energy harvesting.[1] Most of the efforts in the past decade has been devoted to the studies of donor materials, culminating in the development of many electron donors with optimal energy levels, light absorption capacity, etc. for BHJ OSCs.[2] Among these donor materials, porphyrin-based molecular compounds have been widely investigated in view of their extended molecular π-system and structural tunability through peripheral substitution.[3] With respect to electron acceptor materials, fullerene derivatives (e.g., $PC_{61}BM$ and $PC_{71}BM$) are the classical electron acceptor used in BHJ OSCs with power conversion efficiencies (PCEs) over 11%. It is known that the $PC_{71}BM$ can not only efficiently transport the photogenerated mobile electrons by means of percolated pathways to the respective electrode, but also contribute to a large extent to the photocurrent of OSCs at a wavelength of approximately 340 nm, as discussed by Hoppe et al.[4][1b] However, they suffer from a series of limitations including low spectral absorptivity in visible region and difficulty in tuning energy levels as well as propensity to aggregate to undesirably large domains. Accordingly, there have been intense activities directed at developing non-fullerene acceptors with enhanced absorption in the visible and even near-infrared (NIR) region, and adjustable energy levels, resulting in commendable photovoltaic performances.[5] Zhan, et al. reported a series of high-performance nonfullerene acceptors, ITIC-Th, with broad and strong visible light absorption and tunable energy levels, which showed PCEs up to 12.1%, when blended with a wide band gap polymers.[6] And Hou, et al. acheived a record efficiency of 14.4% using IT-4F as non-fullerene acceptor.[7] Another classs of non-fullerene molecular acceptors incorporate perylene diimide (PDI) have also been investigated as it is an excellent electron

transport system.[8] Peng, *et al.* likewise showed a tris-PDI-functionalized 1,3,5-triazine derivative with an efficiency of 9.15%.[9] With a aim to maximize the charge transport property, Henry Yan, *et al.* reported two PDI-tetramers with fused and non-fused structures based on based on a tetrathienylbenzene (TTB) core, leading to a dramatically improved efficiencies up to 10.58%.[10] Porphyrins are a group of naturally occurring intensely colored heterocyclic compounds with 4-meso and 8-β positions readily to be appended with multiple PDI units for high electron mobility. Moreover, porphyrins' characteristic UV-visible spectra consist of two distinct regions: in the near ultraviolet and visible region, which might contribute to the photocurrent in this region. Zhang, *et al.* reported an electron acceptor with four peripheral PDI were conjugated to porphyrin core by alkynyl group, affording a PCE of 7.4% in polymer-based OSC.[11] Although it show a high electron mobility with PBDB-T polymer, the porphyrin core doesn't contribute to the photocurrent so much in the violet region for its much red-shifted absorption due to the good π-conjugation of porphyrin core with four PDIs. Nonetheless, these results have given strong credence to the potential of porphyrin derivatives as acceptors for non-fullerene-based OSCs.

To exploit new PDI-based acceptors with high electron mobility and optimal light harvesting in OSCs, we designed perylenediimide-porphyrin acceptor, 4PDI-ZnP (Scheme 1), in which four PDI units were appended to the porphyrin core via *p*-phenylene linkages. For comparison, 2PDI-ZnP with two PDI units appended was also prepared similarly. The porphyrin core with four *meso*-positions could acts as a peferct scaffold for four PDI units and the excessive steric interferences between the protons of phenylene with those of porphyrin would twist the phenylene bridge out of plane with the porphyrin core, essentially disrupting the π-conjugation of PDI with the porphyrin. This is important in that the electron-rich porphyrin core would adversely affect the electron accepting ability if the PDI moiety and porphyrin core were in full π–conjugation. The situation would be quite different if the

connecting linkage is an acetylene bond[11] where the electron accepting ability of PDI moiety may be suppressed due to the the fully π–conjugation porphyrin core to the PDI unit. At the same time, the disrupted π-conjugation of PDI with the porphyrin would render the new acceptors a undisturbled strong near ultraviolet and violet light response from the poprhyrin core. In addition, twisting effect, would reduce intermolecularly π-π stacking, thus leading to bulk heterojunction with small domain sizes. Accordingly, the acceptor, 4PDI-ZnP with four peripheral PDI moieties, would be expected to be excellent acceptor with optiml visible light repsonse in BHJ OSCs. Moreover, the two acceptors with separated PDI and porhyrin moieties have potential application in single-component BHJ OSCs.

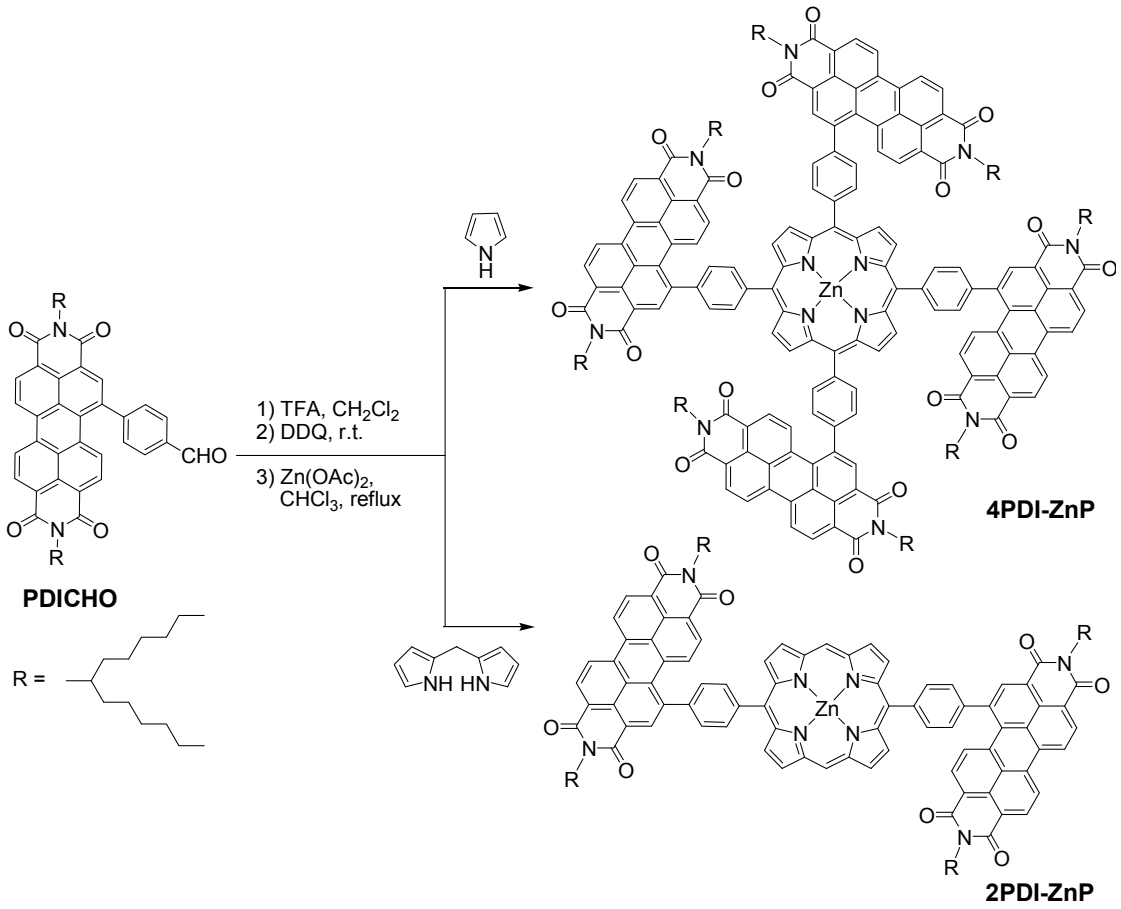

Scheme 1. Syntheses of 2PDI-ZnP and 4PDI-ZnP.

RESULTS and DISCUSSION

Synthesis. The syntheses of 2PDI-ZnP and 4PDI-ZnP were straightforward, involving a trifuoroacetic acid (TFA)-catalyzed condensation of 4-formylphenyl-PDI (PDICHO) with respectively pyrrole and dipyrromethane, followed by reaction with $Zn(OAc)_2$ as illustrated in Scheme 1. The crude products were purified by column chromatography on silica gel. All the compounds were fully characterized by ^1H NMR and matrix-assisted laser desorption/ionization-time of flight mass spectrometry (MALDI-TOF MS). By virtue of severely twisted molecular structures and presence of solubilizing long branched alkyl side-chains, these compounds displayed good solubility in common organic solvents such as toluene, dichloromethane, chloroform, *etc*. In addition, both of these compounds exhibited good thermal stability as their thermogravimetric analyses showing only 5% weight loss at over 400 □C.

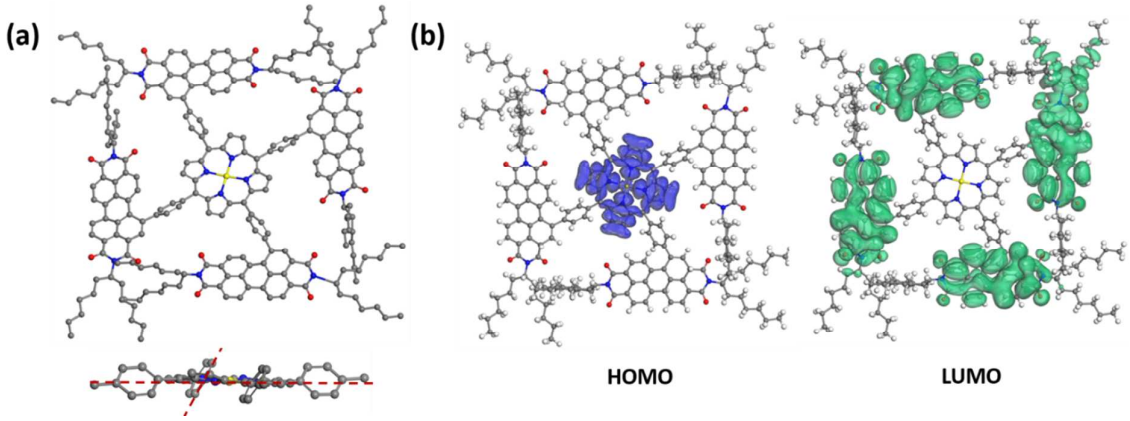

Figure 1. (a) Simulated conformational side-view and partial front-view structures and (b) HOMO/LUMO electron distribution of 4PDI-ZnP.

Theoretical Simulation Studies. Simulation studies on the conformational structures of 2PDI-ZnP and 4PDI-ZnP were carried out using density functional theory (DFT). The results revealed a substantial structural twisting of *p*-phenylene linkage from the relatively planar porphyrin core in these compounds as expected on steric interference considerations (Figure 1a and Figure S1). The structural twisting was far more severe in 4PDI-ZnP with dihedral

angles between the phenylene and porphyrin core ranging from about 51° to about 61° than 2PDI-ZnP, which showed less twisted dihedral angles of about 30°. This was obviously due to the much congested molecular structure of 4PDI-ZnP with four PDI sunstitutions. Accordingly, significant disruption of π-conjugation of PDI moieties with the porphyrin core in these two compounds, particularly 4PDI-ZnP, were to be expected. The consequence of structural twisting are two-fold: (i) the lowest unoccupied molecular orbitals (LUMO) and the highest occupied molecular orbitals (HOMO) are located separately on the different parts of the molecules (Figure 1b); ii) LUMOs of both compounds would be primarily dominated by the contributions from their PDI moieties, thus preserving the electron accepting ability and excellent electron transporting capability of PDI moieties in the compounds; (ii) structural twisting of porphyrin core would avoid the red-shift of its absorption spectrum and render the acceptor specific ultraviolet and violet light repsonse; and (iii) the twisting of PDI moieties would to a large extent restrain the otherwise uncontrolled aggregation of these compounds in their dispersions in polymer donor matrices through intermolecular PDI π-π stacking as for example in the active layers of BHJ OPV devices.

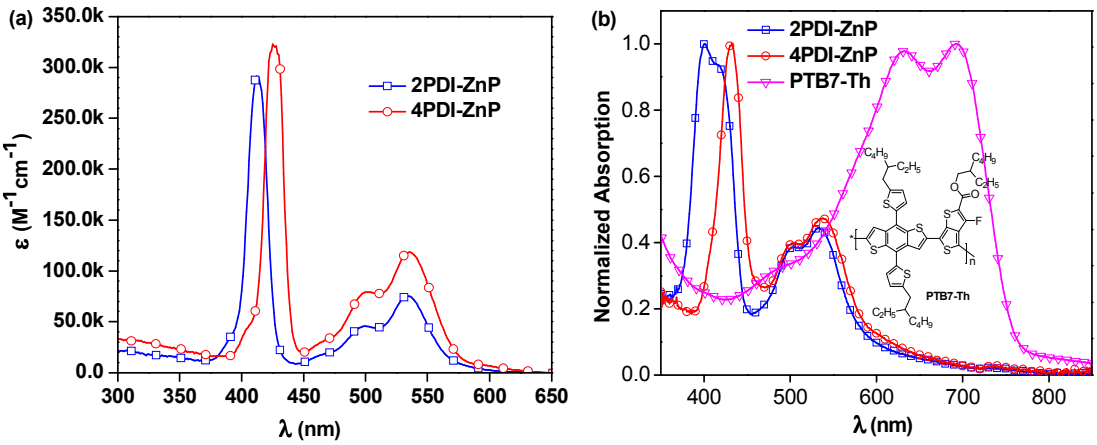

Figure 2. (a) Solution absorption spectra ($CHCl_3$) of 2PDI-ZnP and 4PDI-ZnP; and (b) normalized thin-film absorption spectra of 2PDI-ZnP, 4PDI-ZnP and PTB7-Th.

Absorption Spectral Properties. The UV-visible absorption spectra of 4PDI-ZnP in dilute chloroform ($CHCl_3$) solution exhibited three absorption bands, featuring porphyirn's Soret band at 425 nm and PDI absorptions from 450 to 600 nm, with the Q bands of porphyrin core concealed in the PDI absorption bands. 2PDI-ZnP on the other hand exhibited a blue-shifted peak at 412 nm due to potential H-aggregation and similar PDI absorption peaks at 500 nm and 536 nm (Figure 2, Table 1). In contast, the acceptor reported previously with acetylene linkage between porpyrin and PDI moities showed a much red-shifted Soret band (450–550 nm) and Q bands.[11] The maximum extinction coefficients (ε) for Soret bands of 2PDI-ZnP and 4PDI-ZnP were quite similar, about 2.9×10^5 M^{-1} cm^{-1} and 3.2×10^5 M^{-1} cm^{-1}, respectively. In contrast, the thin-film spectra of 2PDI-ZnP and 4PDI-ZnP showed broader absorption bands, together with approximately 15 nm red-shifts for their Soret bands. These were indicative of relatively weak intermolecular interactions and molecular aggregation in the thin films due to severely twisted molecular structures.[3a] The relatively broad absorptions of these acceptors with high extinction coefficients in both the blue and red regions complemented nicely those of donor polymer, PTB7-Th (Figure 2b)[12] to provide a reasonably wide spectral absoprtion coverage for efficient solar energy harvesting.

Table 1. Photophysical and Electrochemical Properties of 2PDI-ZnP and 4PDI-ZnP.

Compound	λ_{abs} (nm)	E^*_{OX} (eV)[a]	$E_{0\text{-}0}$ (eV)[b]	E_{HOMO}/E_{LUMO} (eV)[c]
2PDI-ZnP	412, 497, 533	−1.05	2.16	−5.94/−3.78
4PDI-ZnP	425, 500, 536	−1.07	2.10	−5.87/−3.77

[a] Oxidation potentials of PDI-porphyrin acceptors were recorded in $CHCl_3$ (1×10^{-4} M) with 0.1 M $TBAPF_6$ as electrolyte. [b] E_{0-0} was determined from the edge of the absorption spectra by 1240/λ. [c] $E_{LUMO} = -(E^*_{OX} + 4.8)$, $E_{HOMO} = -(E_{0\text{-}0} - E_{LUMO})$.

Electrochemical Properties. The lowest unoccupied molecular orbital (LUMO) energy level was calculated to be −3.78 eV for 2PDI-ZnP and −3.77 eV for 4PDI-ZnP from their respective cyclic voltammetric (CV) half-wave reduction potentials in solution (Figure S2, Table 1). Accordingly, the highest occupied molecular orbital (HOMO) energy levels for 2PDI-ZnP and 4PDI-ZnP were respectively estimated to be −5.94 eV and −5.87 eV from their LUMOs and optical bandgaps.[13] Similarly, the CV of PBT7-Th was also recorded in chlorform solution and its HOMO/LUMO energy levels were calculated to be −5.32/−3.69 eV (Figure S3), which are similar to those reported in the literature (HOMO/LUMO = −5.24/−3.66 eV).[12] The large HOMO energy offset between 4PDI-ZnP (or 2PDI-ZnP) and PBT7-Th ensures efficient hole transfer from the electron donor to the electron acceptor. Although the LUMO energy offsets are relatively low, the photoluminescence quenching experiment (Figure S4) and their high performances in BHJ OSCs (see Table 2, *vide infra*) ambiguously sugggested efficient electron transfer from PBT7-Th donor to 4PDI-ZnP (PBT7-Th) acceptor. In addition, a slighter higher LUMO for 4PDI-ZnP than 2PDI-ZnP might attibute to a higher V_{OC} in OSCs with PBT7-Th as donor (see Table 2, *vide infra*).

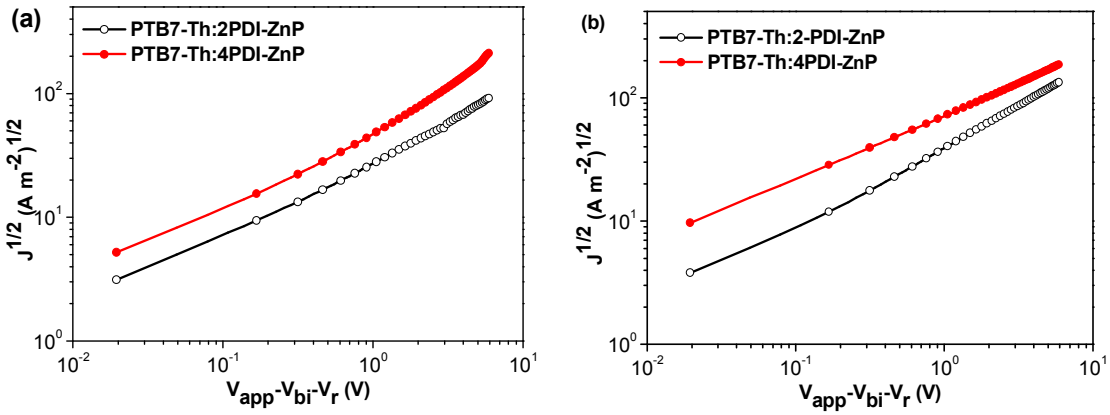

Figure 3. $J^{1/2}$-V curves of the hole-only (a) and electron-only (b) devices.

Charge Transport and Photovoltaic Properties. The electron mobility of 2PDI-ZnP and 4PDI-ZnP in BHJ films with PTB7-Th was measured by space charge limited current (SCLC)

technique using spin-cast thin films from chlorobenzene solutions with 1,8-diiodoctane (DIO) additive. The results showed an electron mobility of 1.34×10^{-4} $cm^2V^{-1}s^{-1}$ and 2.18×10^{-4} $cm^2V^{-1}s^{-1}$ for the BHJ films with respectively 2PDI-ZnP and 4PDI-ZnP acceptors, demonstrating higher electron mobility with higher number of PDI moieties (Figure 3, Table 2). Unlike 2PDI-ZnP:PTB7-Th BHJ film with substantially imbalanced hole (6.37×10^{-5} $cm^2V^{-1}s^{-1}$) and electron (1.34×10^{-4} $cm^2V^{-1}s^{-1}$) mobility, the 4PDI-ZnP:PTB7-Th BHJ film exhibited reasonably balanced hole (3.43×10^{-4} $cm^2V^{-1}s^{-1}$) and electron (2.18×10^{-4} $cm^2V^{-1}s^{-1}$) mobility, an attribute which would be particularly beneficial for exciton dissociation.

Table 2. Charge transport and Photovoltaic Device Parameters[a]

Compound	J_{SC} (mA cm^{-2})	V_{OC} (V)	FF (%)	PCE (%)	μ_h/μ_e ($cm^2V^{-1}s^{-1}$)	R_s ($\Omega\cdot cm^2$)	R_{sh} ($\Omega\cdot cm^2$)
4PDI-ZnP [b]	14.80 ± 0.05	0.87 ± 0.01	62.9 ± 1.4	8.14 ± 0.26	3.43×10^{-4}/ 2.18×10^{-4}	9.3	944.1
4PDI-ZnP [c]	15.35 ± 0.08	0.89 ± 0.01	68.8 ± 1.6	9.40 ± 0.24	–	7.9	1476.9
2PDI-ZnP [b]	12.66 ± 0.06	0.84 ± 0.01	49.3 ± 2.1	5.22 ± 0.31	6.37×10^{-5}/ 1.34×10^{-4}	14.7	316.3
2PDI-ZnP [c]	13.00 ± 0.01	0.85 ± 0.01	54.7 ± 1.9	6.04 ± 0.34	–	12.4	586.4

[a] Each value is averaged from 10 devices with standard deviation after ±. [b] Device based on ITO/ZnO/ZrAcac/PTB7-Th:Acceptor/MoO3/Ag; [c] Device based on ITO/ZnO/PNDIT-F3N-Br/PTB7-Th:Acceptor/MoO3/Ag.

Experimental BHJ OSC devices with an active layer of PTB7-Th and 2PDI-ZnP or 4PDI-ZnP using a device configuration of ITO/ZnO/Zirconium acetylacetonate(ZrAcac)/PTB7-Th:Acceptor/MoO_3/Ag were characterized under AM 1.5 illumination (detailed device fabrication in Supporting Information). The *J-V* curves and external quantum efficiency (EQE) spectra for the optimized devices are presented in Figure S5 (device parameters in

Table 2). The optimized BHJ OSC devices with an active layer of PTB7-Th:2PDI-ZnP exhibited a moderate PCE of 5.53%, with V_{OC} of 0.85 V, J_{SC} of 12.72 mA cm^{-2} and FF of 51.4%. In sharp contrast, the devices with PTB7-Th:4PDI-ZnP as active layer afforded a very higher PCE of 8.40%, with an improved V_{OC} of 0.88 V, J_{SC} of 14.85 mA cm^{-2} and FF of 64.3%. The measured EQEs of optimized devices showed broad spectral response in the 300–800 nm, which was consistent with the complementary absorption spectral properties of donor and acceptor in the active layer films (Figure 2b). Furthermore, a high EQE of over 80% was observed for the 4PDI-ZnP devices, as compared to an EQE value of about 78% for the 2PDI-ZnP devices. The integration of the EQE spectra corresponds to J_{SC} value of 12.22 and 14.51 mA cm^{-2} for the optimal devices of PTB7-Th:2PDI-ZnP and PTB7-Th:4PDI-ZnP, respectively, which are comparable to the J_{SC} values measured in the *J-V* curves. The performance of the PBT7-Th:4PDI-ZnP device was also consistent with its higher shunt resistance (R_{sh}) of 944.1 Ω·cm^2 and lower series resistance (R_s) of 9.3 Ω·cm^2 (Table 2), which were closely related to J_{SC} and FF, and led to better device performance without significant charge recombination under both AM 1.5 illumination and weak light irradiations.

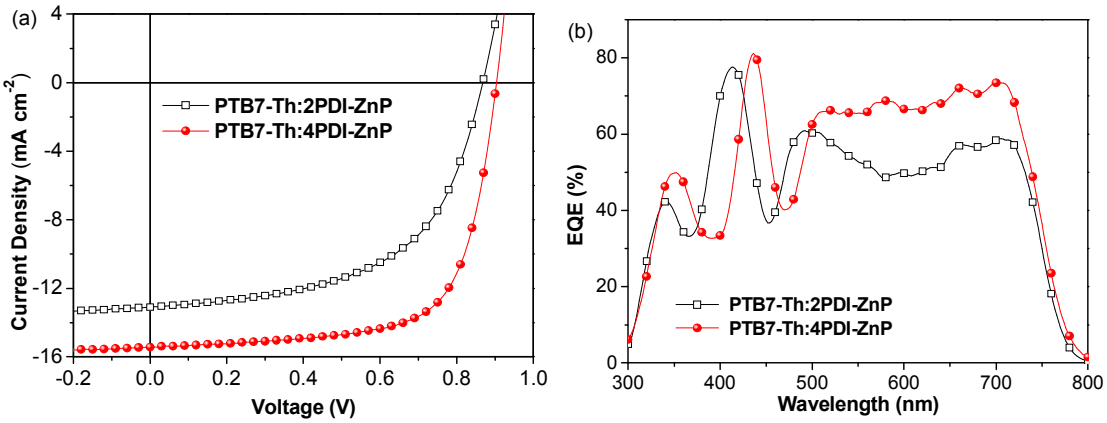

Figure 4. *J-V* (a) and EQE (b) of BHJ OSCs based on device of ITO/ZnO/PNDIT-F3N-Br/PTB7-Th:Acceptor/MoO_3/Ag under AM 1.5G illumination at 100 mW cm^{-2}.

We further used PNDIT-F3N-Br instead of ZrAcac as electron transport layer (ETL) in BHJ OSCs device.[14] The *J-V* curves for the optimal devices are presented in Figure 4a (device parameters in Table 2). The optimal BHJ OSC devices with an active layer of PTB7-Th:2PDI-ZnP exhibited a enhanced PCE of 6.38%, with V_{OC} of 0.86 V, J_{SC} of 13.10 mA cm^{-2} and FF of 56.6%. And the devices with PTB7-Th:4PDI-ZnP as active layer also afforded a enhanced PCE of 9.64%, with an improved V_{OC} of 0.90 V, J_{SC} of 15.43 mA cm^{-2} and FF of 69.4%. The measured EQEs of optimized devices showed similar broad spectral response in the 300–800 nm (Figure 4b). And the integration of the EQE spectra corresponds to J_{SC} value of 12.87 and 15.12 mA cm^{-2} for the optimal devices of PTB7-Th:2PDI-ZnP and PTB7-Th:4PDI-ZnP, respectively, which are comparable to the J_{SC} values measured in the *J-V* curves. The enhancement of the devices is mainly due to highly conductive PNDIT-F3N-Br as ETLs with reduced ohmic loss for electron transport and extraction. The results are consistent with its further increased shunt resistance (Rsh) of 1476.9 Ω·cm2 and lower series resistance (Rs) of 7.9 Ω·cm2 (Table 2). In addition, the device stability was tested under heating at 100 °C. After 24 hours, the PCE retained around 75% and 51% of the initial value for the devices of PTB7-Th:2PDI-ZnP and PTB7-Th:4PDI-ZnP (Figure S6), respectively.

Recently, Li and his co-workers resported a series of “double-cable” conjugated polymers, which contain electron-donating poly(benzodithiophene) (BDT) as linear conjugated backbone for hole transport and pendant electron-deficient perylene bisimide (PBI) units for electron transport, and applied them in efficient single-component polymer solar cells with PCEs up to 4.18%.[15] Herein, the two acceptors with disrupted conjugation between the PDI moieties and porphyrin core were tested in single-component organic solar cells based on the inverted configuration (ITO/ZnO/PNDIT-F3N-Br/Acceptor/MoO_3/Ag) or the conventional one (ITO/PEDOT:PSS/Acceptor/PFN/Al). The *J-V* and EQE curves of the optimized devices are respectively presented in Figure S7 (device parameters in Table S2). Due to difficuly of

controlling the morphology of the small molecules, the devices showed very poor performances with PCE of 0.27% and 0.43% in invetical devices, and 0.25% and 0.39% in conventional devices for 2PDI-ZnP and 4PDI-ZnP, respectively. The measured EQEs of the devices clearly indicated the significant light-harvesting contribution of the porphyrin core typically in a range of 300–450 nm. We measured the CV of single N,N'-1-(tridecan-7-yl)-perylenebis(dicarboximide) (PDI) molecule and calcualted its HOMO/LUMO energy levels to be −6.08/−3.80 eV, which is well alligned with the HOMO/LUMOs (−5.06/−2.10 eV) of zinc(II) tetraphenylporphyrin (ZnTPP) reported.[16] Therefore the electron transfer from porphyrin core to PDI moieties is reasonbale due to decoupling of the PDI moieties with the porphyrin core. We believe, by rationally designing the electron-withdrawing and electron-donating moieties, as well as linkage between them, an optimized nanophase separation in single-component small molecules can be realized, and therefore high-performance single-component BHJ OSCs can be achieved.

To study the exciton dissociation and carrier collection process, the charge dissociation probability $P(E, T)$, $P(E, T) = J_{ph}/J_{sat}$, was investigated according to the reported methods.[17] The photocurrent density J_{ph} ($J_{ph} = J_L - J_D$), where J_L and J_D are the current density of the devices under illumination and dark, respectively, as a function of effective voltage V_{eff} ($V_{eff} = V_0 - V$), where V_0 is the voltage at $J_{ph} = 0$ was measured. If $J_{ph} = J_{sat}$ at high reverse voltage ($V_{eff} > 2$ V), all the photo-generated excitons would be dissociated to free charge carriers and collected by the electrodes (recombination would be suppressed by high internal electric field).[18] As shown in Figure S8, the J_{ph} of PTB7-Th:2PDI-ZnP and PTB7-Th:4PDI-ZnP devices showed substantial differences. The PTB7-Th:4PDI-ZnP devices displayed a flat plateau at a region of relatively low V_{eff}, and did not saturate at high V_{eff} region even up to 2.5 V. The calculated charge dissociation probability $P(E, T)$, estimated from the ratio of J_{ph}/J_{sat}, for the PTB7-Th:4PDI-ZnP devices was 91%, indicating efficient exciton dissociation. On

the contrary, the PTB7-Th:2PDI-ZnP devices afforded a lower $P(E, T)$ value of 82%, suggesting less effective exciton dissociation and serious charge recombination. Accordingly, a higher number of PDI units in the acceptor had a positive effect of promoting exciton dissociation and reducing charge recombination, thus contributing to enhanced photovoltaic performance.

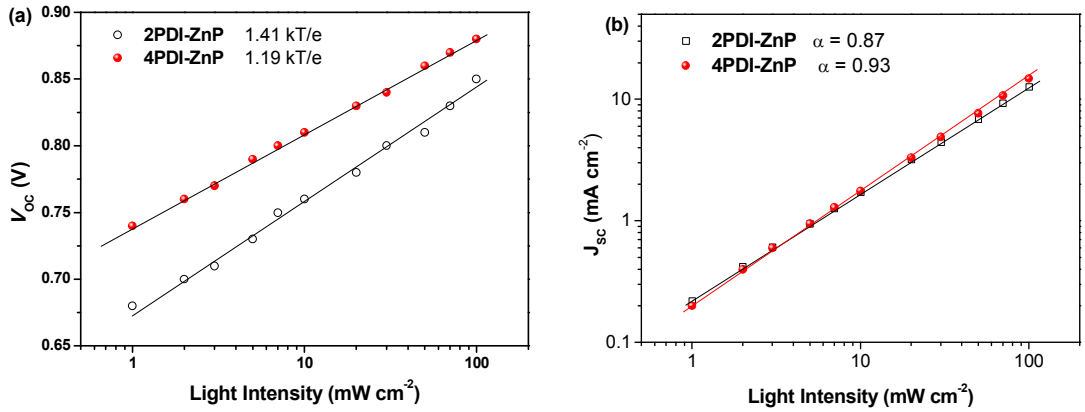

Figure 5. (a) V_{OC} and (b) J_{SC} of the optimal devices versus light intensity.

We also investigated J_{SC} as a function of illumination intensity in logarithmic scale to gain further insight into the exciton recombination (Figure 5). If the slope of the curve reaches 1, it implies that bimolecular recombination is not a crucial loss mechanism at the short-circuit point. In the case of PTB7-Th:2PDI-ZnP and PTB7-Th:4PDI-ZnP devices, the α value was estimated to be respectively 0.87 and 0.93, indicating that the PTB7-Th:4PDI-ZnP devices had a weaker bimolecular recombination than that of PTB7-Th:2PDI-ZnP devices. The dependence of V_{OC} on light intensity (P_{light}) can be used to describe the order of recombination processes in the BHJ film. The semi-logarithmic plot of V_{OC} depends linearly on light intensity with a slope of kT/q for bimolecular recombination. A slope greater than kT/q points toward trap-assisted recombination, where k, T, and q are the Boltzmann constant, temperature in Kelvin, and the elementary charge.[19] For our evaluation, the optimal devices of PTB7-Th:2PDI-ZnP and PTB7-Th:4PDI-ZnP were measured with a slope of 1.41 kT/q

and 1.19 kT/q, respectively, demonstrating that a reduced trap-assisted recombination was realized in the PTB7-Th:4PDI-ZnP devices (Figure 5a).

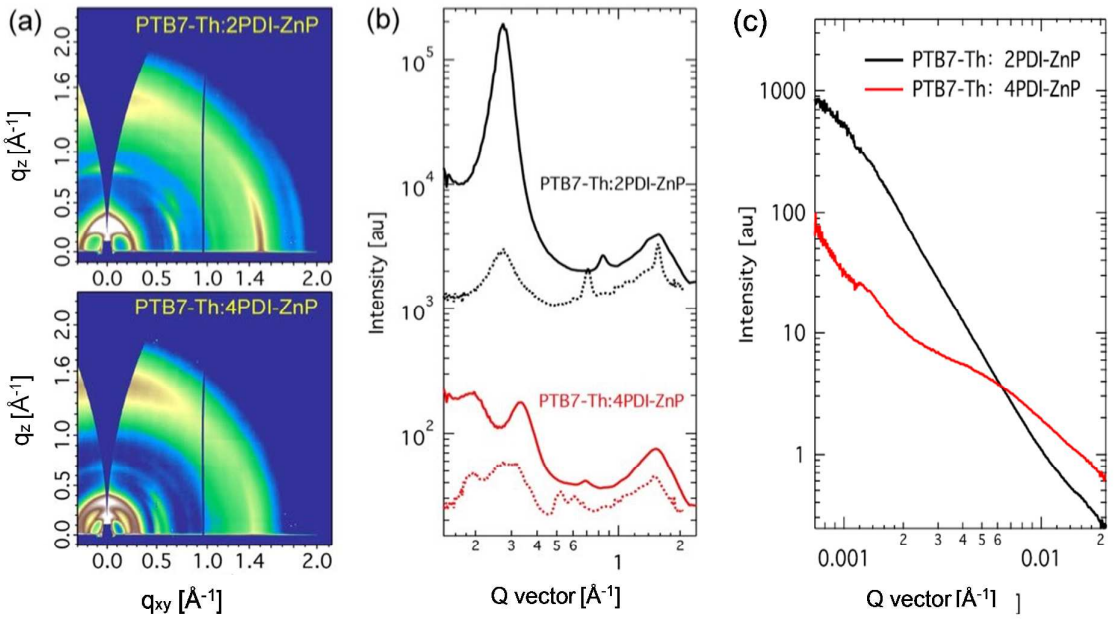

Figure 6. (a) Grazing incidence X-ray diffraction patterns, (b) line-cut profiles (solid line: out-of-plane, dotted line: in-plane) and (c) resonant soft x-ray scattering of BHJ films.

Morphological Properties. The structural orders of PTB7-Th:acceptor BHJ films were investigated using grazing incidence wide-angle x-ray diffraction (GIWAXS) (Figure 6a, b). PTB7-Th is a well studied polymer that showed face-on orientation in both neat and BHJ thin films with well-recorded packing features. The scattering features of the PTB7-Th:2PDI-ZnP BHJ film were dominated by the acceptor component. A sharp (100) peak was seen in out-of-plane direction at 0.27 $Å^{-1}$ with a crystal coherence length (CCL) of 21.6 nm. The packing orientation showed high edge-on preference, yet a broad π-π stacking peak was also noted. In the in-plane direction, a sharp π-π stacking peak at 1.56 $Å^{-1}$ with a CCL of 12.1 nm and a relatively weak (100) peak were noted. The broad out-of-plane π-π stacking peak was contributed from both PTB7-Th and 2PDI-ZnP, which could not be fully disentangled. These

results showed poor ordering of 2PDI-ZnP acceptor in the BHJ film, which led to poorer charge carrier ransport and photovoltaic power conversion efficiency.

On the other hand, the PTB7-Th:4PDI-ZnP BHJ films showed quite different scattering features. The low q region showed multiple scattering peaks at 0.19 and 0.33 $Å^{-1}$ in in-plane direction coming from 4PDI-ZnP, and a (100) scattering at 0.27 $Å^{-1}$ attributable to PTB7-Th, agreeing well with previous report. The out-of-plane direction showed packing features of 4PDI-ZnP, similar to that in in-plane directions with much lower scattering intensities as compared to the 2PDI-ZnP:PTB7-Th composite film. No sharp π-π stacking was observed from 4PDI-ZnP in in-plane direction, but a quite broad and intense peak in out-of-plane direction at 1.53 $Å^{-1}$ was noted. These results were in strong agreement with the suggestion that the molecularly twisted structure of 4PDI-ZnP had effectively suppressed uncontrolled aggregation, which would have adversely impacted exciton dissociation and charge carrier transport effcienies.The phase separation of the BHJ films were further studied by resonant soft x-ray scattering (RSoXS) at 287 eV. As seen from scattering profiles (Figure 6c), 2PDI-ZnP:PTB7-Th showed a high scattering intensity in low q region with quite steep decay line as a result of large phase separation or surface roughness, which deteriorated the charge separatoin and collection as well as device performance. This feature was seen in both off-edge and in-edge photon energies. On the other hand, 4PDI-ZnP:PTB7-Th showed a low intensity low q scattering but broad hump from 0.003-0.02 $Å^{-1}$, indicating a broad length scale of phase separation at 30-200 nm length scales. The small length-scale phase separation would be critical in driving charge separation and collection as well as promoting large internal surface area, leading to improved device current. Though less ordered, the 4PDI-ZnP:PTB7-Th film with better π-π stacking orientation had helped improve charge transport and collection and thus a high FF.

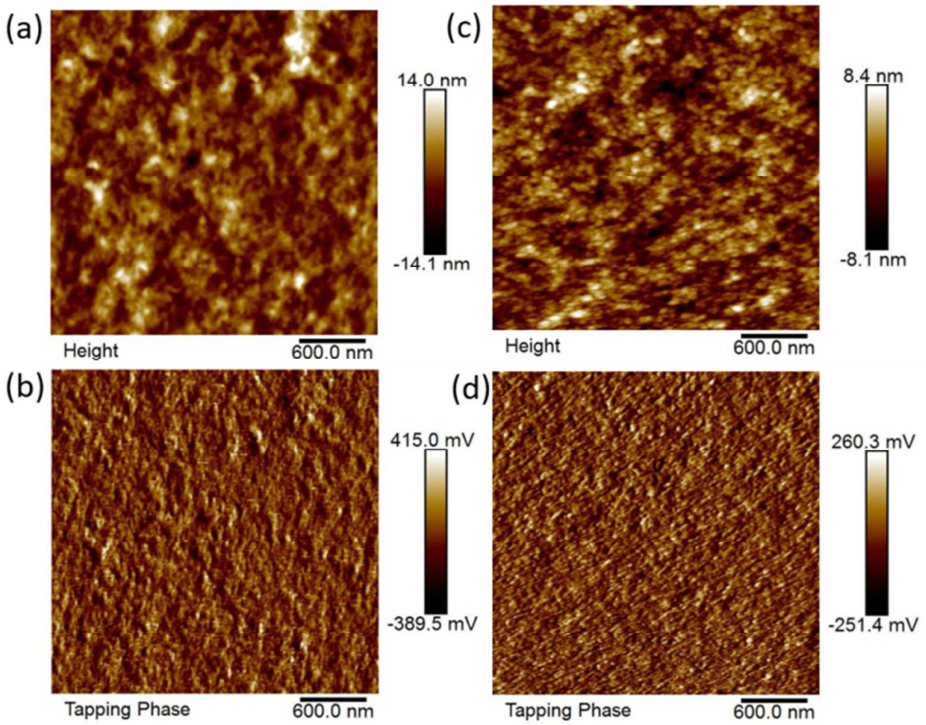

Figure 7. AFM height and phase images of PTB7-Th:2PDI-ZnP (a, b) and PTB7-Th:4PDI-ZnP (c, d).

4PDI-ZnP/2PDI-ZnP:PTB7-Th BHJ films were also characterized using atomic force microscopy (AFM) (Figure 7). The results showed that the number of PDI units in the acceptors had a definitive effect on the film morphology. Specifically, the 4PDI-ZnP:PTB7-Th film exhibited a more homogeneous morphology with a root-mean-squared (RMS) surface roughness of 2.4 versus 3.5 nm for the 2PDI-ZnP:PTB7-Th film. In addition, the topographic patterns for the 2PDI-ZnP:PTB7-Th film displayed a rough nodular character, indicative of significantly large extent of phase separation which was unfavorable for exciton diffusion,[20] and would lead to lower J_{SC}. In contrast, a lesser extent of phase separation and smoother surface morphology were observed for the 4PDI-ZnP:PTB7-Th film, and this would explain for the observed higher J_{SC} and higher PCE arising from enhanced exciton diffusion/dissociation and charge carrier transport. Optimal crystalline domains and phase

separation in the active layer are beneficial to charge carrier transport and for achieving high J_{SC}, while uncontrolled aggregation would lower the J_{SC} and PCE.[21]

CONCLUSIONS

We have demonstrated that PDI-functionalized porphyrin derivatives are potentially good electron acceptor materials in combination with an appropriate polymer donor in BHJ OSCs for their high electron mobility and optimal light-harvesting. The number of PDI moiety in the acceptors has a profound effect on their photovoltaic performances as it impacts the spectral absorptivity, molecular structural twisting, active layer morphology, exciton dissociation and carrier transport, etc., and thus PCE as a whole. Accordingly, 4PDI-ZnP acceptor, in conjunction with PBT7-Th donor, has afforded a optimal PCE of 9.64%, which is hitherto benchmark photovoltaic performance for PDI-porphyrin acceptor/PBT7-Th system. It should be noted that the porphyrin core not only acted as scaffold for PDI moieties, but also contributed the light-harvesting in near-ultraviolet and violet regions, which is unambiguously demonstrated in single-component BHJ OSCs based on the two acceptors. We believe that with further process and solar cell structural optimization, higher PCE could be acheived with these acceptors in combination wiht a more appropriate donor.

ASSOCIATED CONTENT

Supporting Information. The method of device fabrication, the synthesis and characterizations of porphyrin acceptors 2PDI-ZnP and 4PDI-ZnP.

Notes

The authors declare no competing financial interest.

ACKNOWLEDGMENT

This work was supported by the Hong Kong Research Grants Council (HKBU 22304115-ECS and and C5015-15GF), Areas of Excellence Scheme ([AoE/P-03/08]), Hong Kong Baptist University (FRG1/15-16/052, FRG2/16-17/024) and The Science, Technology and Innovation Committee of Shenzhen Municipality (JCYJ20150630164505504) for support. TPR were supported by the U.S. Office of Naval Research under contract N00014-15-1-2244. Portions of this research were carried out at beamline 7.3.3 and 11.0.1.2 at the Advanced Light Source, and Molecular Foundry, Lawrence Berkeley National Laboratory, which was supported by the DOE, Office of Science, and Office of Basic Energy Sciences.

REFERENCES

[1] H. Kang, G. Kim, J. Kim, S. Kwon, H. Kim, K. Lee, *Adv. Mater.* **2016**, *28*, 7821-7861.

[2] X. X. Liu, H. J. Chen, S. T. Tan, *Renew. Sust. Energ Rev.* **2015**, *52*, 1527-1538.

[3] a) L. G. Xiao, S. Chen, K. Gao, X. B. Peng, F. Liu, Y. Cao, W. Y. Wong, W. K. Wong, X. J. Zhu, *ACS Appl. Mater. Interfaces* **2016**, *8*, 30176-30183; b) H. D. Wang, L. G. Xiao, L. Yan, S. Chen, X. J. Zhu, X. B. Peng, X. Z. Wang, W. K. Wong, W. Y. Wong, *Chem. Sci.* **2016**, *7*, 4301-4307; c) J. Kesters, P. Verstappen, M. Kelchtermans, L. Lutsen, D. Vanderzande, W. Maes, *Adv. Energy Mater.* **2015**, *5* (13), 1500218; d) L. Bucher, N. Desbois, P. D. Harvey, G. D. Sharma, C. P. Gros, *Sol. RRL* **2017**, *1* (12), 1700127 (1-26); e) H. M. Qin, L. S. Li, F. Q. Guo, S. J. Su, J. B. Peng, Y. Cao, X. B. Peng, *Energy Environ. Sci.* **2014**, *7*, 1397-1401; f) L. Bucher, L. Tanguy, D. Fortin, N. Desbois, P. D. Harvey, G. D. Sharma, C. P. Gros, *ChemPlusChem* **2017**, *82*, 625-630; g) S. Chen, L. Yan, L. G. Xiao, K. Gao, W. Tang, C. Wang, C. H. Zhu, X. Z. Wang, F. Liu, X. B. Peng, W. K. Wong, X. J. Zhu, *J. Mater. Chem. A* **2017**, *5*, 25460-25468; h) N. F. Montcada, S. Arrechea, A. Molina-Ontoria, A. I. Aljarilla, P. de la Cruz, L. Echegoyen, E. Palomares, F. Langa, *Org. Electron.* **2016**, *38*, 330-336.

[4] L. Derue, O. Dautel, A. Tournebize, M. Drees, H. L. Pan, S. Berthumeyrie, B. Pavageau, E. Cloutet, S. Chambon, L. Hirsch, A. Rivaton, P. Hudhomme, A. Facchetti, G. Wantz, *Adv. Mater.* **2014**, *26*, 5831-5838.

[5] a) C. Q. Yan, S. Barlow, Z. H. Wang, H. Yan, A. K. Y. Jen, S. R. Marder, X. W. Zhan, *Nat. Rev. Mater.* **2018**, *3,* 18003; b) C. B. Nielsen, E. Voroshazi, S. Holliday, K. Cnops, B. P. Rand, I. McCulloch, *J. Mater. Chem. A* **2013**, *1*, 73-76.

[6] P. Cheng, G. Li, X. W. Zhan, Y. Yang, *Nat. Photonics* **2018**, *12*, 131-142.

[7] S. Q. Zhang, Y. P. Qin, J. Zhu, J. H. Hou, *Adv. Mater.* **2018**, *30,* 1703973.

[8] a) D. Sun, D. Meng, Y. H. Cai, B. B. Fan, Y. Li, W. Jiang, L. J. Huo, Y. M. Sun, Z. H. Wang, *J. Am. Chem. Soc.* **2015**, *137*, 11156-11162; b) D. Meng, D. Sun, C. M. Zhong, T. Liu, B. B. Fan, L. J. Huo, Y. Li, W. S. Jiang, H. S. Choi, T. Kim, J. Y. Kim, Y. M. Sun, Z. H. Wang, A. J. Heeger, *J. Am. Chem. Soc.* **2016**, *138*, 375-380.

[9] Y. W. Duan, X. P. Xu, H. Yan, W. L. Wu, Z. J. Li, Q. Peng, *Adv. Mater.* **2017**, *29* (7), 1605115 (1-6).

[10] J. Q. Zhang, Y. K. Li, J. C. Huang, H. W. Hu, G. Y. Zhang, T. X. Ma, P. C. Y. Chow, H. Ade, D. Pan, H. Yan, *J. Am. Chem. Soc.* **2017**, *139*, 16092-16095.

[11] A. D. Zhang, C. Li, F. Yang, J. Q. Zhang, Z. H. Wang, Z. X. Wei, W. W. Li, *Angew. Chem. Int. Edit.* **2017**, *56*, 2694-2698.

[12] Z. G. Wang, X. P. Xu, Z. J. Li, K. Feng, K. Li, Y. Li, Q. Peng, *Adv. Electron. Mater.* **2016**, *2* (6), 1600061 (1-7).

[13] H. R. Lin, S. S. Chen, H. W. Hu, L. Zhang, T. X. Ma, J. Y. L. Lai, Z. K. Li, A. J. Qin, X. H. Huang, B. Z. Tang, H. Yan, *Adv. Mater.* **2016**, *28*, 8546-8551.

[14] Z. H. Wu, C. Sun, S. Dong, X. F. Jiang, S. P. Wu, H. B. Wu, H. L. Yip, F. Huang, Y. Cao, *J. Am. Chem. Soc.* **2016**, *138*, 2004-2013.

[15] G. T. Feng, J. Y. Li, F. J. M. Colberts, M. M. Li, J. Q. Zhang, F. Yang, Y. Z. Jin, F. L. Zhang, R. A. J. Janssen, C. Li, W. W. Li, *J. Am. Chem. Soc.* **2017**, *139*, 18647-18656.

[16] J. N. Clifford, E. Martinez-Ferrero, A. Viterisi, E. Palomares, *Chem. Soc. Rev.* **2011**, *40*, 1635-1646.

[17] Z. Li, J. D. A. Lin, H. Phan, A. Sharenko, C. M. Proctor, P. Zalar, Z. H. Chen, A. Facchetti, T. Q. Nguyen, *Adv. Funct. Mater.* **2014**, *24*, 6989-6998.

[18] Y. Z. Lin, Q. He, F. W. Zhao, L. J. Huo, J. Q. Mai, X. H. Lu, C. J. Su, T. F. Li, J. Y. Wang, J. S. Zhu, Y. M. Sun, C. R. Wang, X. W. Zhan, *J. Am. Chem. Soc.* **2016**, *138*, 2973-2976.

[19] a) A. K. K. Kyaw, D. H. Wang, C. Luo, Y. Cao, T. Q. Nguyen, G. C. Bazan, A. J. Heeger, *Adv. Energy Mater.* **2014**, *4* (7), 1301469; b) H. Azimi, A. Senes, M. C. Scharber, K. Hingerl, C. J. Brabec, *Adv. Energy Mater.* **2011**, *1*, 1162-1168.

[20] P. Cheng, L. Ye, X. G. Zhao, J. H. Hou, Y. F. Li, X. W. Zhan, *Energy Environ. Sci.* **2014**, *7*, 1351-1356.

[21] X. Zhang, Z. H. Lu, L. Ye, C. L. Zhan, J. H. Hou, S. Q. Zhang, B. Jiang, Y. Zhao, J. H. Huang, S. L. Zhang, Y. Liu, Q. Shi, Y. Q. Liu, J. N. Yao, *Adv. Mater.* **2013**, *25*(40), 5791-5797.

Table of Contents

Phenylene-bridged perylenediimide-porphyrin acceptors for non-fullerene organic solar cells